Spherical probes and quantized vortices: Hydrodynamic formalism and simple applications*

K. W. Schwarz
Department of Physics and The James Franck Institute, The University of Chicago, Chicago, Illinois 60637
(Received 1 July 1974)

The velocity field of an ideal fluid in the presence of a moving spherical boundary and a vortex line of arbitrary configuration is found, and the hydrodynamic force acting on the sphere determined. Using this formalism, one may compute the motion of the sphere and the vortex line in the general case where the sphere has inertia and is subject to externally applied forces. The resulting algorithm can be utilized to study the complicated hydrodynamic interactions between charge carriers and quantized vortices in superfluid helium. As simple examples of the application of the hydrodynamic formalism, the force exerted on a moving sphere by an instantaneously rectilinear vortex is evaluated, and the interaction of a vortex ring with a fixed sphere is considered.

I. INTRODUCTION

The theory of vortex filaments in an ideal fluid has attracted renewed interest in recent years as it has become apparent that quantized vortices in superfluid helium represent a very good physical realization of the ideal vortex-filament concept. Perhaps the most convincing demonstration of this has been the discovery of quantized vortex rings and the observation that they behave in accord with the predictions of classical hydrodynamics,[1] but many other elegant experiments have also exhibited effects arising from the presence of quantized vortices under various conditions. Among such experiments, some involve presumed arrangements of vortex lines and bounding surfaces of sufficiently high symmetry to permit at least an approximate analytical treatment of the relevant vortex dynamics. For example, a rotating bucket of superfluid is generally assumed to be filled with a forest of rectilinear vortex lines directed along the axis of rotation with a density $2\Omega/\kappa_0$, where Ω is the angular speed of rotation and $\kappa_0 = h/m$ is the quantum of circulation. Experiments such as the measurement of the attenuation of second sound by the vortex lines,[2] or the oscillating-disk measurements of Hall,[3] presumably do not involve sufficient local vortex line distortions to destroy this high degree of symmetry. Similarly, experiments on the energy loss of large quantized vortex rings,[1,4] on vortex rings normally incident on a plane boundary,[5,6] and on rings passing through holes in a plane boundary[7,8] have been analyzed on the assumption that the system in question remains axially symmetric.

Many of the most interesting experiments, however, deal with vortex-line dynamical effects which, while qualitatively transparent and easily formulated in principle, involve configurations too complicated for an analytical treatment. For example, charge carriers moving across a rotating bucket can be trapped on the rectilinear vortex lines filling the bucket, because of the strong short-range hydrodynamic interaction between the probe and the lines.[9] The charge carriers can to a good approximation be thought of as very small spheres, and the relevant hydrodynamic problem is therefore the encounter of a sphere with an initially straight vortex line [Fig. 1(a)]. Experiments have also been performed in which a beam of quantized vortex rings is passed through a rotating bucket[10] or through a second beam of rings.[11] In this case, one must consider a vortex ring incident on an initially straight vortex line [Fig. 1(b)], or on another ring. Yet another related type of problem arises when one considers the creation of quantized vortex rings by rapidly moving charge carriers.[12,13] Various hypothetical descriptions of the actual creation process have been proposed,[13,14] and most recently it has been shown that a generalized Landau argument based on energy and momentum conservation yields critical velocities for ring creation that are in qualitative agreement with experiment.[15] This argument predicts that the ring should first appear girdling the spherical charge carrier, roughly as in Fig. 1(c), and therefore the subsequent hydrodynamic development of such an initial configuration must be considered in working out the implications of the model. Finally, neutral vortex rings have been detected by letting them pick up a bare charge.[16] Thus one is led to consider a sphere and a vortex ring incident on each other [Fig. 1(d)].

The situations indicated in Fig. 1 will develop in rather complicated ways with time. In addition, a realistic interpretation of the various relevant experiments must take account of the random changes which arise as the ever-present elementary excitations scatter off the vortex core and the charge carrier. It is therefore not surprising that the many interesting experiments relating to these somewhat messy kinds of problems have not yet

been subjected to extensive theoretical analysis. Two relatively simple special cases have been considered in detail. The interaction of a vortex ring with a rectilinear vortex line in the absence of normal-fluid effects has been calculated on the basis of the classical hydrodynamic formalism, and good agreement with experiment has been obtained.[10] At the opposite extreme, the trapping and evaporation of charge carriers by rectilinear vortex lines has been rather successfully explained[9,17] on the basis of the phenomenological assumption that the hydrodynamic interaction between the carrier and the line can be represented by an effective potential well, with the charge carriers thermally diffusing into and out of this well. Such a picture seems reasonable in the limit where the carrier mean free path against excitation scattering is very short compared to the size of the well, but it is expected to break down at temperatures below ~1.5 °K.

It is possible to develop a somewhat more unified approach to this general class of problems, an approach based on the ideas that up to a certain point ideal fluid dynamics is an adequate approximation for describing the interactive motion of charge carriers and quantized vortex lines on the microscopic level, and that the effect of elementary excitation scattering is to give rise to suitable random instantaneous changes in the velocity of the charge carrier and in the vortex line configuration. Let us consider the time development of some initially specified configuration, such as those in Fig. 1, in the presence of elementary excitations. The sphere is assumed to have mass M, and will respond not only to the forces exerted on it by the fluid, but also to an external force $e\vec{\mathcal{E}}$ when an electric field is present. Suppose now that one describes the instantaneous configuration of the system in terms of some set of parameters, such as the coordinates of a sufficient number of points on the vortex line and the position and velocity of the sphere. For convenience of discussion these parameters can be thought of as defining a space. A given initial configuration defines a point in this space, and the subsequent hydrodynamic motion of the system can be represented as a path in this space. The totality of possible time developments for all initial conditions is then given by a system of paths in the parameter space (Fig. 2). In order to generalize this schematic picture to include the effects of the elementary excitations, one may make the reasonable assumption that the relevant scattering events take place on a very short time scale compared to the times over which significant hydrodynamical changes occur. The effect of a scattering event is then to "instantaneously" modify the configuration of the system, causing it to jump to a different path in parameter space. Thus a system starting at A in Fig. 2 will no longer follow the path to B, but, as it suffers random changes due to scattering, will instead undergo a kind of Brownian motion among the various paths in parameter space. In a typical experiment many such "systems" are present simultaneously, a situation which can be represented in terms of a distribution of points in the parameter space, with each point undergoing such a motion.

To treat a given problem of interest in terms of this generalized kinetic model, one needs both to work out the various hydrodynamic paths that the system can follow in parameter space and to determine the rate at which the system is scattered

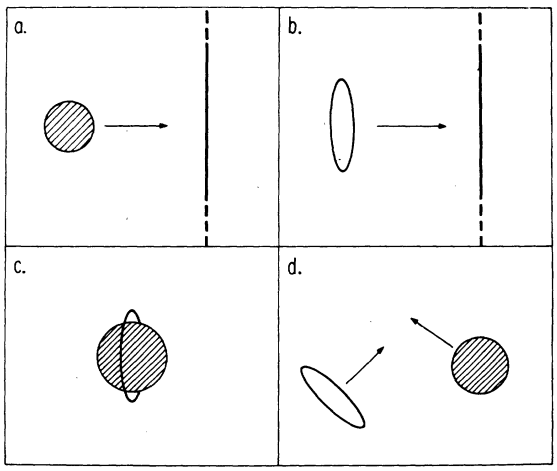

FIG. 1. Encounters between spheres, vortex rings, and vortex lines that are of interest in the interpretation of various experiments discussed in the text.

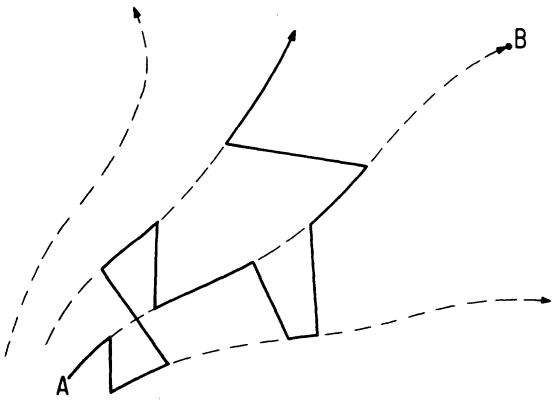

FIG. 2. Schematic rendering of the generalized Brownian motion undergone by a sphere-line hydrodynamic system in the presence of elementary excitations.

from one configuration to another. Even in the absence of elementary excitation scattering, the task of calculating the time development of systems like those in Fig. 1 seems quite formidable, and the main point of the present paper is to show how it can be accomplished. Before launching into such detailed considerations, however, a brief discussion of some of the qualitative ideas that enter the overall picture many prove useful. The kinds of hydrodynamic processes of interest to us are various types of encounters between vortex rings, rectilinear vortex lines, and spheres. In terms of the example of Fig. 1(a), consider an initial state where the sphere and the line are far apart, but where the subsequent motion is such as to bring them into proximity. Depending on the exact initial conditions, the system will develop in one of two very different ways. On the one hand, the approach of the two objects may involve some mildly eccentric vortex distortions and sphere motions, but eventually they will again separate in an unambiguous fashion. Such an interaction will be called a nonentangling encounter. In contrast, one finds that for other initial conditions there is a very violent interaction from which the two objects never again emerge with separate identities, at least within the context of the ideal-fluid formalism. We call this an entangling encounter. Encounters between a ring and a fixed sphere are analyzed in detail in Sec. III. The important qualitative idea which comes out of these calculations is that if a configuration develops such that a vortex core comes very close to another vortex core, or to its own image in a surface, a complicated irreversible vortex tangle forms very quickly. If such a close approach does not occur, local vortex distortions remain moderate and the encounter is nonentangling. In practice, it appears that one can usually draw a very sharp distinction between configurations that will develop into an entangling encounter and those that will separate.

The distinction between entangling and nonentangling encounters can be incorporated into our more general picture of a kinetic process occurring in a suitable parameter space. The above discussion implies that there is a sharply defined region of this space which has the property that, once the system enters it, an irreversible entangling process takes place (Fig. 3). Since the primary effect detected in the experiments under consideration is the occurrence of some drastic local interaction between two kinds of objects,[18] one may assume as a reasonable working hypothesis that such an interaction corresponds microscopically to what we have called an entangling encounter. The experimentally observed trapping or annihilation rate is then the rate at which the points in parameter space enter the entangling region, either hydrodynamically or by elementary excitation scattering. One should note, however, that hydrodynamic calculations dealing with idealized vortex filaments in an ideal fluid are not capable of predicting the ultimate result of an entangling encounter. It is therefore more strictly correct to interpret the flux into the entangling region as providing an upper limit to the rate at which the experimentally detected trapping or annihilation processes can occur. In addition, the nature of the final state of a carrier trapped on a vortex, or the mechanism by which such a charge again manages to escape from the vortex, seems for now to be beyond the scope of our calculations.

The qualitative hydrodynamic features of the problem aside, it is also relevant to inquire briefly into the nature of the stochastic effects introduced by excitation scattering. The simplest case to consider is the scattering of a phonon, roton, or He^3 impurity by a charge carrier, such an event merely giving rise to an impulsive change in the velocity of the carrier. The effect arising from the scattering of an excitation by a vortex is somewhat less obvious. When an excitation scatters from a localized region of the fluid, a nonconservative force is exerted on the fluid in this region. It has been shown by Huggins[19] that such a force gives rise to a shift in the "center of mass" of the local vorticity distribution, a shift which proceeds with a velocity $\vec{V}$ given by

$$\rho\vec{V}\times\vec{\kappa}_0=\vec{F}\,, \tag{1}$$

where $\vec{\kappa}_0$ is the total vector circulation about the vortex and $\vec{F}$ is the total force per unit length of the vortex. An event in which an impulse

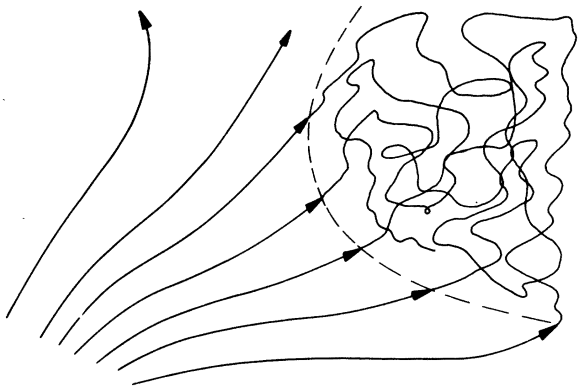

FIG. 3. Schematic rendering of the existence of an entangling region in the hydrodynamic parameter space of a sphere-line system.

$$\vec{I} = \Delta L \int \vec{F}\, dt \tag{2}$$

is given to a local region of length ΔL of the vortex is therefore accompanied by an impulsive displacement $\vec{\delta}$ of the vorticity distribution. $\vec{I}$ is of course just equal to the momentum lost by the elementary excitation as it is scattered, so that

$$\rho \vec{\delta} \times \vec{\kappa}_0 = \hbar(\vec{k} - \vec{k}')/\Delta L \ . \tag{3}$$

A complete formalism in terms of incident wave packets can be worked out, but the important qualitative idea is that excitations scattering off the vortices give rise to stochastic fluctuations in the *configuration* of the vortices.

When a situation involving both charge carriers and vortices is considered, the stochastic fluctuations of the system points in parameter space will more generally consist of changes both in the carrier velocity and in the vortex configuration. To develop the appropriate generalized kinetic theory, one needs the transition rate $\Gamma(P_i \to P_i')$, defined as the probability per unit time that a system with parameters P_i will be scattered to the state P_i' by the elementary excitations that are present. The calculation of $\Gamma(P_i \to P_i')$ appears at present to be feasible only when the wavelength of the excitations is small compared to both the spatial separations between the interacting objects and the minimum radius of curvature of any vortex line. In this limit, the elementary excitations scatter independently off the charge carriers and the effectively straight vortex lines, and Γ may be determined from the differential cross sections for such relatively simple processes. In particular, our understanding of how the excitations scatter off the charge carriers has advanced to the point[20,21] where it can easily be incorporated quantitatively into our general framework. Attempts to calculate differential cross sections for the scattering of phonons, rotons, and He^3 impurities by rectilinear vortices have also met with some success,[22,23] and further progress can be expected. One can, at least, set up reasonable approximate models for these processes.

The considerations given above indicate the current limitations and the possible areas of success for a microscopic treatment of carrier-line and line-line interactions which takes realistic account of both hydrodynamic and stochastic effects. Briefly, one may hope to determine the rate at which strong encounters will occur in a given experiment, provided the elementary excitations are such that certain simplifying approximations can be made. As a first step in this direction, the remainder of the present paper will be devoted to a consideration of the relevant hydrodynamic problems.

II. HYDRODYNAMIC FORMALISM

A. Instantaneous velocity field

The properties of an ideal incompressible fluid are determined by[24]

$$\partial \vec{v}/\partial t + (\vec{v} \cdot \nabla)\vec{v} = -\nabla P/\rho \ , \tag{4}$$

$$\nabla \cdot \vec{v} = 0 \ , \tag{5}$$

along with the condition that at any boundary the normal component of the fluid velocity equal the normal component of the boundary velocity. The velocity field generated by a vorticity distribution $\vec{\omega}(\vec{r}') = \nabla \times \vec{v}$ in the absence of boundaries is given by

$$\vec{v}_I(\vec{r}) = \frac{1}{4\pi} \int \frac{(\vec{r} - \vec{r}') \times \vec{\omega}(\vec{r}')}{|\vec{r} - \vec{r}'|^3}\, dV' \ . \tag{6}$$

In superfluid helium, vorticity exists only in the form of quantized vortex lines. Except when evaluating the self-induced velocity of the lines, we shall approximate the vortex lines as filaments,

$$\vec{\omega}(\vec{r}) = \kappa_0 \delta(\vec{r}' - \vec{r}_l) \ , \tag{7}$$

where κ_0 is the quantum of circulation. The finite size of the core ($a \sim 1$ Å) does not affect the accuracy of the calculations, provided that the radius of curvature of the line and its distance from any surface remain comparatively large. As these quantities approach a, results based on Eq. (7) become more qualitative, and no hydrodynamic significance can be attached to configurations with characteristic distances of the order of a or less. In practice the approximation of Eq. (7) does not introduce any important uncertainties into the predictions of the theory.

In the event that only vortex lines are present, the velocity field may be evaluated immediately from Eqs. (6) and (7). If, however, a spherical boundary representing a moving carrier is also present, the velocity field takes the form

$$\vec{v} = \vec{v}_l + \nabla\Phi_b + \nabla\Phi_u \ , \tag{8}$$

where

$$\Phi_u = -\tfrac{1}{2} b^3 \vec{U} \cdot (\vec{r} - \vec{r}_s)/|\vec{r} - \vec{r}_s|^3 \tag{9}$$

is the scalar potential of the moving sphere alone, and Φ_b is the potential of the field needed to satisfy the boundary conditions on the sphere. In Eq. (9), b denotes the radius of the sphere, $\vec{U}$ its velocity, and $\vec{r}_s$ the position of its center.

The boundary generated field must be found by solving

$$\nabla^2 \Phi_b = 0 \tag{10}$$

subject to the condition that at $|\vec{r} - \vec{r}_s| = b$,

$$(\vec{v}_l + \nabla \Phi_b) \cdot \hat{n} = 0 \,. \tag{11}$$

The approach most convenient for our purposes is to find the contribution $d\Phi_b$ which arises from the $d\vec{v}_l$ generated by an arbitrary element $\kappa_0 \, d\vec{l}$ of the vortex line. The total solution is then a simple integral over such contributions, which is easily evaluated numerically for an arbitrary vortex line configuration.[25] Let the vector from the center of the sphere to the line element define the polar axis of a spherical coordinate system, and the direction of $d\vec{l}$ perpendicular to this axis define the zero of the azimuthal angle (Fig. 4). Then Eq. (11) becomes

$$\left. \frac{\partial d\Phi_b}{\partial r} \right|_{r=b} = -\frac{\kappa_0 \, dl_\perp}{4\pi} \frac{R \sin\vartheta \sin\phi}{(R^2 + b^2 - 2Rb\cos\vartheta)^{3/2}} , \tag{12}$$

where R denotes the distance of the line element from the center of the sphere.

This is now a standard problem. From the known solutions of Eq. (10) in spherical coordinates,

$$d\Phi_b = \frac{\kappa_0 \, dl_\perp}{4\pi} \frac{R \sin\phi}{r} \sum_{n=1}^{\infty} B_n \frac{P_n^1(\cos\vartheta)}{r^n} , \tag{13}$$

where P_n^1 is the associated Legendre function of the first kind, and

$$B_n = \frac{n + \frac{1}{2}}{n(n+1)^2} \, b^{n+2} \int_0^\pi \frac{P_n^1(\cos\vartheta) \sin^2\vartheta \, d\vartheta}{(R^2 + b^2 - 2Rb\cos\vartheta)^{3/2}} . \tag{14}$$

The integral may be evaluated in closed form by expressing P_n^1 in terms of Legendre polynomials and making use of known integral formulas.[26] One obtains the result

$$d\Phi_b = \frac{\kappa_0 \, dl_\perp}{4\pi} \frac{b}{rR} \sin\phi \sum_{n=1}^{\infty} \frac{1}{n+1} \left(\frac{b^2}{rR} \right)^n P_n^1(\cos\vartheta). \tag{15}$$

The velocity potential Φ_b and the associated velocity field $\vec{v}_b$ may now be generated for an arbitrary vortex-line configuration by dividing the line up into elements and using Eq. (15). This procedure is readily reduced to a routine numerical computation.

B. Development in time

The velocity field is totally determined by the instantaneous position and velocity of any boundaries and by the instantaneous distribution of vorticity. If the rate of change of these quantities can be expressed in terms of the velocity field, the time development of the system can then be determined by an iterative procedure. The rate of change of the vorticity distribution is determined by Kelvin's circulation theorem,[27] which states that a vortex filament will move with the material particles of the fluid. The determination of the time development of a system in which only vortices are present (e.g., ring-line encounters) is then particularly simple, since the fluid velocity at the vortex core evaluated from Eq. (6) determines the motion of the vortex. In practice a slight difficulty arises in considering the effect of a vortex on itself: if the vortex is treated as an idealized filament of finite strength, the contribution of a point $\vec{r}_l'$ on the line to the velocity at a point $\vec{r}_l$ diverges logarithmically as $\vec{r}_l'$ approaches $\vec{r}_l$.[28] To evaluate the self-induced velocity correctly, it is necessary to take account of the distribution of vorticity within the core of the vortex. Provided that the core radius is small compared to the radius of curvature of the vortex, this can be done by introducing a suitable cutoff parameter,[29] confining the integration to those parts of the vortex filament for which $|\vec{r}_l - \vec{r}_l'| \geq a$. The cutoff parameter can be interpreted roughly as being equal to the radius of the vortex core,[8] and has the value $a \approx 1.3$ Å for a quantized vortex.[1,30] The dynamics of, say, a ring-line encounter can then be worked out readily.[10]

The time development of a system containing

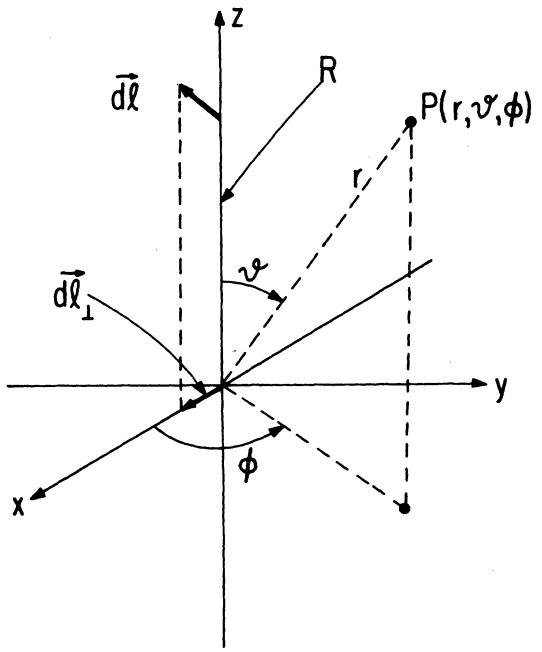

FIG. 4. Coordinate system for the determination of the boundary field $d\Phi_b$.

quantized vortices and a *fixed* spherical boundary can also be treated in a straightforward way, it only being necessary to include the effects of the boundary field $\vec{v}_b$ on the motion of the vortices. A more complicated situation arises in the general case of interest where one lets the sphere have mass M and be acted upon by an external field $e\vec{\mathcal{E}}$. Then

$$M\dot{\vec{U}} = e\vec{\mathcal{E}} + \vec{F}(\dot{\vec{U}}) , \tag{16}$$

where $\vec{F}$ is the force exerted by the fluid on the sphere. As indicated, $\vec{F}$ will depend on the acceleration $\dot{\vec{U}}$ of the sphere, as well as on the velocity field. It is not *a priori* obvious that the rate of change of $\vec{U}$ can be related in a simple way to the instantaneous velocity field, and hence that an iterative determination of the time development of the system is possible. However, it is well known[31] that for a sphere in an infinite fluid with no vorticity the contribution of the acceleration reaction to $\vec{F}$ can be subsumed into an effective mass, and we shall find that this simplification also applies to the present case.

The force exerted by the fluid on the sphere is

$$\vec{F} = -\int_{\text{sphere}} p\hat{n}\, dS , \tag{17}$$

where p is the pressure and the normal $\hat{n}$ is taken into the fluid. The flow in the immediate neighborhood of the sphere is postulated to be irrotational, and thus the pressure may be obtained from Bernoulli's law,

$$\partial\Phi/\partial t + \tfrac{1}{2}v^2 + p/\rho = \text{constant} , \tag{18}$$

where Φ is the scalar velocity potential. Hence

$$\vec{F} = \rho \int_{\text{sphere}} \left(\frac{\partial\Phi}{\partial t} + \tfrac{1}{2}v^2\right)\hat{n}\, dS , \tag{19}$$

where the integral over $\partial\Phi/\partial t$ must of course be interpreted in the sense

$$\int_{\text{sphere}} \frac{\partial\Phi}{\partial t}\,\hat{n}\, dS = \lim_{S\to\text{sphere}} \int_S \frac{\partial\Phi}{\partial t}\,\hat{n}\, dS , \tag{20}$$

with S lying everywhere in the fluid.

The force may be expressed in terms of the vortex, boundary, and moving-sphere fields by inserting $\Phi = \Phi_l + \Phi_b + \Phi_u$ and $\vec{v} = \vec{v}_l + \vec{v}_b + \vec{v}_u$ into Eq. (19). The term $\partial\Phi_l/\partial t$ arises from the convection of the vorticity distribution by the local velocity field $\vec{v}_l + \vec{v}_b + \vec{v}_u$. One may conveniently divide $\partial\Phi_b/\partial t$ into a contribution $\partial\Phi_b(A)/\partial t$, which comes from the time-dependence of Φ_l, plus a contribution $\partial\Phi_b(B)/\partial t$, which arises because of the motion of the spherical boundary. $\partial\Phi_u/\partial t$ also splits into two parts, one arising from the acceleration $\dot{\vec{U}}$ of the sphere and the other from its motion. These distinctions allow us to state a number of simplifications of Eq. (19). First, the term in $\partial\Phi_u/\partial t$ which depends on $\dot{\vec{U}}$ is the only such term in the total force. Since Φ_u represents simply a moving sphere alone, this contribution is just the usual acceleration reaction of a sphere in an infinite fluid, and can be folded into an effective mass for the sphere. Equation (16) then becomes

$$M_{\text{eff}}\,\dot{\vec{U}} = e\vec{\mathcal{E}} + \vec{F} , \tag{21}$$

where

$$M_{\text{eff}} = M + \tfrac{2}{3}\pi\rho b^3 , \tag{22}$$

and $\vec{F}$ is now the force felt by a *steadily* moving sphere. Second, the part of $\partial\Phi_u/\partial t$ that arises from the motion of the sphere combines with the term $\frac{1}{2}v_u^2$ to give zero, since a steadily moving sphere in an infinite fluid experiences no net force. Third, the surface integral over the combination $\partial\Phi_l/\partial t + \partial\Phi_b(A)/\partial t$ yields $2\pi\rho b^3(\partial/\partial t)\,\vec{v}_l(\vec{r}_s, t)$, where $\vec{v}_l(\vec{r}_s, t)$ denotes the vortex-generated field at the center of the sphere. Finally, the combination $\partial\Phi_b(B)/\partial t + \vec{v}_u\cdot(\vec{v}_l + \vec{v}_b)$ integrates identically to zero. The proof of the last two assertions is somewhat complicated and is therefore deferred to an Appendix. With these simplifications, the equation of motion of the sphere now takes the form

$$M_{\text{eff}}\,\dot{\vec{U}} = e\vec{\mathcal{E}} + 2\pi\rho b^3 \frac{\partial}{\partial t}\,\vec{v}_l(\vec{r}_s, t) + \tfrac{1}{2}\rho \int_{\text{sphere}} (\vec{v}_l + \vec{v}_b)^2 \hat{n}\, dS . \tag{23}$$

The results given above provide a straightforward algorithm for computing the interactive motion of a system composed of a spherical probe subject to external forces and a quantized vortex line of arbitrary configuration. At a given instant in time, the rate of change of coordinates describing the location of the line is given by the instantaneous velocity field at the line, and this can be determined by the method of Section II A. The rate of change of the sphere position is just given by the velocity $\vec{U}$, and the rate of change of $\vec{U}$ is given by Eq. (23), the right hand side of which depends on the instantaneous line configuration and the rate of change of this configuration, both of which are already known. Thus the rate of change of all of the system parameters can be evaluated in terms of their instantaneous values, and a step-by-step integration of the time development of the system is possible. While such an approach lacks the elegance of analytical methods, it is well suited to the kind of problems of interest here.

In general, the integration of the motion of the system is tedious, and leads to rather complicated results. We therefore limit the present discussion to two relatively simple examples which nevertheless provide some useful physical insights. We first evaluate the force exerted by an instantaneously rectilinear vortex on a moving sphere. It will be of interest to compare the resulting interaction with the simplified effective potential used by Donnelly and Roberts[9] in their stochastic model. We shall also investigate the behavior of vortex rings incident on a fixed spherical boundary, in order to elucidate how an entangling encounter arises.

III. SIMPLE APPLICATIONS

A. Force exerted by a rectilinear vortex

From Eq. (23), one can identify two contributions to the hydrodynamic force felt by a sphere. Rubinow and Keller[32] have in fact evaluated the $(\vec{v}_l + \vec{v}_b)^2$ integral for the case of a rectilinear vortex, and they find

$$\vec{F} = -\frac{\rho\kappa_0^2}{2\pi}\frac{b^3\vec{r}}{r^3}\sum_{n=1}^{\infty}\frac{2^{2n}(n!)^2}{(2n)!\,(n+1)}\left(\frac{b}{r}\right)^{2n-1}, \quad (24)$$

where $\vec{r}$ is the radius vector from the line to the sphere (Fig. 5). This radial attractive force is plotted as curve 1 in Fig. 6.

Further contributions to the force, which have not yet been discussed in the literature, arise from the convective motion of the vortex line. For a straight line the self-induced motion is of course zero, but the fields $\vec{v}_b$ and $\vec{v}_u$ will cause motion of the line and hence contribute to $(\partial/\partial t)\vec{v}_l(\vec{r}_s, t)$. The primary effect of $\vec{v}_b$ is to cause the near parts of the line to move around the sphere (i.e., in the $+\hat{y}$ direction in Fig. 5). The resulting rotation of $\vec{v}_l(\vec{r}_s, t)$ generates a force contribution which is primarily repulsive in the radial direction and of much shorter range than that given by Eq. (24). Curve 2 in Fig. 6 demonstrates the effect of this correction.

The force arising from the convection of the line by $\vec{v}_u$ depends in a complicated way on the direction and magnitude of the sphere velocity. We note that this force is velocity dependent and in general not radial, and that it can be made as large as one pleases by making $\vec{U}$ large. As a particular example, curves 3 and 4 in Fig. 6 show the azimuthal component of the force experienced by spheres with radii of 17 Å and 6 Å, respectively, when they are approaching the line at a speed of 5 m sec^{-1}. In terms of the geometry of Fig. 5, this force acts in the $-\hat{y}$ direction.

In an experiment where charge carriers approach initially straight vortex lines, one will of course expect the lines to deform during the time of strong interaction. However, in the high temperature regime roton scattering will presumably act to damp out such deformations, at least until the

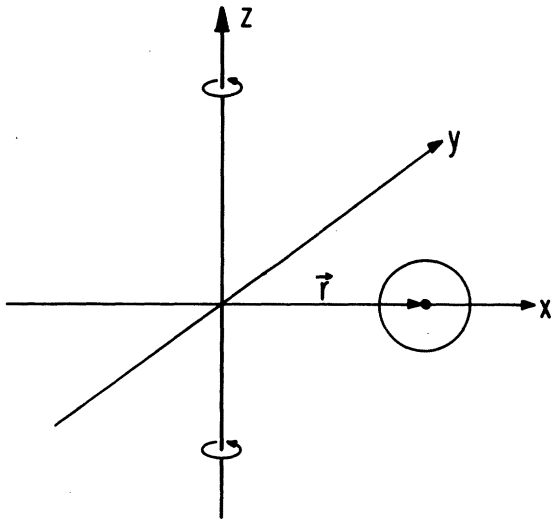

FIG. 5. Geometry used in the determination of the force exerted on a sphere by a straight vortex line.

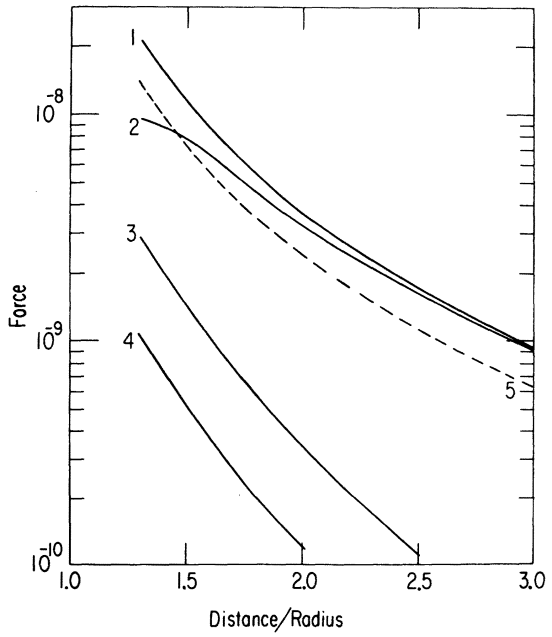

FIG. 6. Forces exerted on a sphere by a straight vortex line. Curve 1 is calculated from Eq. (24). Curve 2 is the radial attractive force felt by a stationary sphere. Curves 3 and 4 show the azimuthal forces felt by spheres of radii 17 and 6 Å, respectively, when they approach the line at a speed of 5 m sec^{-1}. Curve 5 is the force law assumed by Donnelly and Roberts.

probe approaches the line very closely. The force felt by the carrier will then consist of the strong radial attraction shown as curve 2 in Fig. 6, plus a relatively small nonradial velocity-dependent correction of the type shown by curves 3 and 4. It is interesting to note that Donnelly and Roberts[9] have used the radial, velocity-independent interaction shown by curve 5 in developing their high-temperature theory of charge trapping by vortex lines. One may conclude from Fig. 6, that for $r \geq 1.3b$, their assumptions are in quite good agreement with the exact hydrodynamic calculations.

B. Vortex ring incident on a fixed sphere

Vortex rings incident on a spherical surface with a radius of 17 Å were investigated in some detail. In the numerical calculations the ring is broken up into initially equal line segments (Fig. 7), the corresponding boundary fields $d\vec{v}_b$ are found, and the fluid velocity at the midpoint of every line segment is then evaluated. These midpoints are then displaced by an amount proportional to the local velocity, a new set of line elements is constructed, and so forth. The effect of a line element on itself is obtained by analytically integrating Eq. (6) over a circular line element constructed as shown in Fig. 7. The resulting local contribution is

$$\vec{v}_I = \hat{z}\,(\kappa_0/4\pi R)[\ln(R/a) + \ln\theta]\ , \tag{25}$$

where $\hat{z}$ is the unit vector out of the plane of the figure, R is the local radius of curvature, the term $\ln(R/a)$ arises from the core cutoff, and the term $\ln\theta$ arises from the cutoff at the ends of the element. A test of these procedures was made by numerically studying the time development of isolated vortex rings. Results were entirely satisfactory, yielding stable ring propagation velocities differing by only a few percent from the analytical prediction

$$v = (\kappa_0/4\pi R)[\ln(8R/a) - \tfrac{1}{4}]\ . \tag{26}$$

The geometrical framework of the calculation is shown in Fig. 8. The y axis is defined as being in the initial direction of motion of the vortex ring and passing through the center of the sphere. The initial displacement of the ring center from the y axis is taken along the x axis. The configuration then always remains symmetrical with respect to reflection about the x-y plane.

Results for a ring of radius 17 Å incident on a sphere of radius 17 Å are shown in Fig. 9. A ring with impact parameter zero [Fig. 9(a)] passes smoothly around the sphere, growing and shrinking as it does so under the influence of the boundary field $\vec{v}_b$. With an impact parameter of 2 Å [Fig. 9(b)], the ring still passes around the sphere but becomes somewhat distorted in doing so and will oscillate gently as it moves off into the distance. The situation changes drastically when the impact parameter is increased to 4 Å [Fig. 9(c)]. Now the part of the ring which approaches nearest to the surface is suddenly captured by the velocity field of its image and wound around the sphere. Such irreversible entangling behavior continues to characterize the interaction as the impact parameter is increased further, and in Fig. 9(d) one sees that it occurs even for rings which have been aimed to miss the sphere entirely.

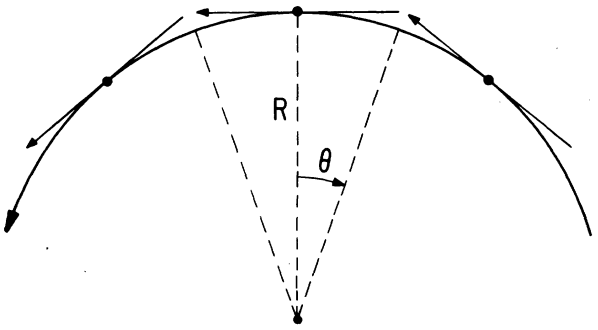

FIG. 7. Division of a vortex ring into equal line segments.

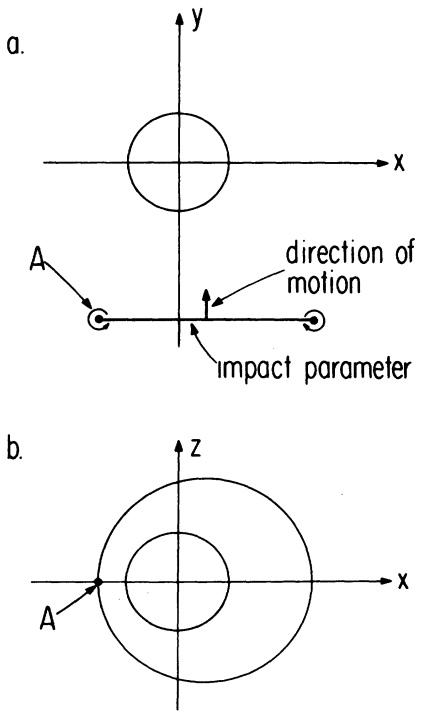

FIG. 8. Geometrical framework for the calculation of an encounter between a vortex ring and a fixed sphere.

Rings aimed to miss the sphere by an amount slightly larger than in Fig. 9(d) will suffer only very slight distortions and propagate out to infinity.

The genesis of an entangling interaction is readily understood by considering the behavior of a vortex ring moving parallel to a boundary coincident with the y-z plane. In Fig. 10 the reader is asked to visualize the ring as curving in from large x below the plane of the figure, passing through the plane of the figure at the point of closest approach, and curving back out to large x as it comes out of the plane of the figure. For a plane boundary, the boundary-generated velocity field may be found by the method of images. Clearly, the effect of the image ring is to retard the self-induced motion of that part of the ring closest to the surface, so that an initially plane ring A becomes distorted to shape B. The essential point is that the distorted part of the ring now has a self-induced velocity component *into* the surface. It will consequently approach the surface more closely (as in C), the effect of the image field will be increased, and so on. The result is that the image field "grabs" the nearest part of the ring and runs off with it along the surface, as shown in D. The time development of such a pronounced loop lying along the surface soon becomes hopelessly complicated, resulting in a vortex tangle localized at the surface. Ultimately, of course, the ideal fluid approximation breaks down.

Behavior very similar to that displayed in Fig. 9 is observed in the case of much larger, slower incident rings (Fig. 11), except that the cross section for the ring passing around the sphere without entangling becomes increasingly large as the ring size increases. It is of some interest to inquire how well a simple geometrical model for the entangling cross section agrees with the more complicated hydrodynamic results. Naively, one might assume that an entangling event will occur only if the ring is initially aimed so that some part of it will intersect the surface of the sphere. Then

$$\sigma_t = \pi(b+R)^2 \quad R \leq b$$
$$= 4\pi bR \quad R \geq b \,, \tag{27}$$

where b is the sphere radius and R is the ring radius. Figure 12 shows the ratio of the entangling cross section obtained from our hydrodynamic calculations to the geometrical cross section of Eq. (27). The agreement is in fact seen to be reasonably good over the range of R that we have studied.

To conclude this section we point out that the idealization made in replacing the finite core by a vortex filament at the center of the core does not lead to any major inaccuracies in the computed entangling cross sections. It is clear from Figs. 9 and 11 that entangling is initiated when the vortex

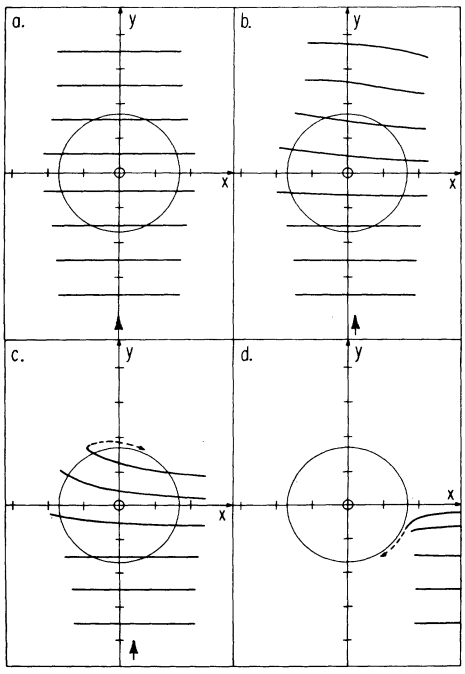

FIG. 9. 17-Å ring incident on 17-Å sphere, for various impact parameters. Projection of the ring onto the x-y plane [as in Fig. 8(a)] is plotted at various stages in the development of the ring.

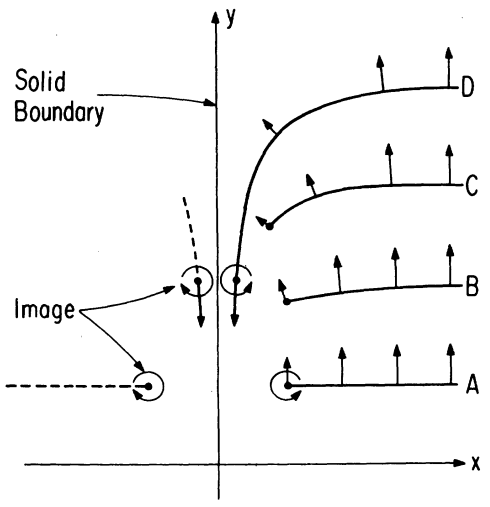

FIG. 10. Development of a ring moving parallel to a plane boundary. Projection of the near part of the ring onto the x-y plane is plotted at various stages in the development of the ring.

is still about 4 Å away from the surface. At this distance the vortex-filament approximation is still quite accurate.

ACKNOWLEDGMENTS

I should like to thank Professor Ian Lerche, Professor J. Pedlosky, and Professor Dieter Forster for their helpful comments.

APPENDIX

In this Appendix is sketched the proof of the two lemmas used in Sec. II B. If the velocity potential Φ_I is expanded about the origin of the sphere at $t=0$,

$$\Phi_I = \sum_{n=1}^{\infty} \sum_{m=-n}^{n} c_{n,m}(t) r^n Y_n^m(\vartheta, \phi), \tag{A1}$$

then $\Phi_b(A)$, corresponding to the boundary potential generated by a stationary sphere, is given by

$$\Phi_b(A) = \sum_{n=1}^{\infty} \sum_{m=-n}^{n} \frac{n}{n+1} c_{n,m}(t) b^n \left(\frac{b}{r}\right)^{n+1} Y_n^m(\vartheta, \phi). \tag{A2}$$

At $r=b$,

$$\Phi_I + \Phi_b(A) = \sum_{n=1}^{\infty} \sum_{m=-n}^{n} \frac{2n+1}{n+1} c_{n,m}(t) b^n Y_n^m(\vartheta, \phi). \tag{A3}$$

Applying Bernoulli's law and integrating over the surface of the sphere, one obtains[32]

$$F_x = \tfrac{1}{2}\rho b^2 \sum_{n=1}^{\infty} \sum_{m=-n}^{n} b^{2n-1} \frac{n(2n+1)(2n+3)}{n+1} (-1)^m B_n^m (c_{n,m} c_{n+1,-m-1} - c_{n,-m} c_{n+1,m+1})$$
$$+ (\tfrac{3}{2}\pi)^{1/2} \rho b^3 \left(\frac{d}{dt} c_{1,-1} - \frac{d}{dt} c_{1,1}\right),$$
$$F_y = \frac{1}{2i} \rho b^2 \sum_{n=1}^{\infty} \sum_{m=-n}^{n} b^{2n-1} \frac{n(2n+1)(2n+3)}{n+1} (-1)^m B_n^m (c_{n,m} c_{n+1,-m-1} + c_{n,-m} c_{n+1,m+1}) \tag{A4}$$
$$+ \frac{1}{i} (\tfrac{3}{2}\pi)^{1/2} \rho b^3 \left(\frac{d}{dt} c_{1,-1} + \frac{d}{dt} c_{1,1}\right),$$
$$F_z = \rho b^2 \sum_{n=1}^{\infty} \sum_{m=-n}^{n} b^{2n-1} \frac{n(2n+1)(2n+3)}{n+1} (-1)^m A_n^m c_{n,m} c_{n+1,-m} + (3\pi)^{1/2} \rho b^3 \frac{d}{dt} c_{1,0},$$

where

$$A_n^m = [(n-m+1)(n+m+1)/(2n+1)(2n+3)]^{1/2}$$
$$B_n^m = [(n+m+1)(n+m+2)/(2n+1)(2n+3)]^{1/2}. \tag{A5}$$

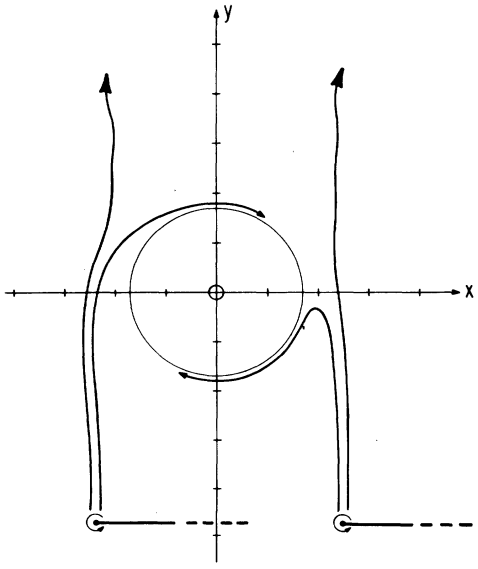

FIG. 11. 80-Å ring incident on 17-Å sphere, for various impact parameters. The path of the near edge of the ring (point A in Fig. 8) is given here. Note that in all cases the ring extends far beyond the right-hand edge of the figure.

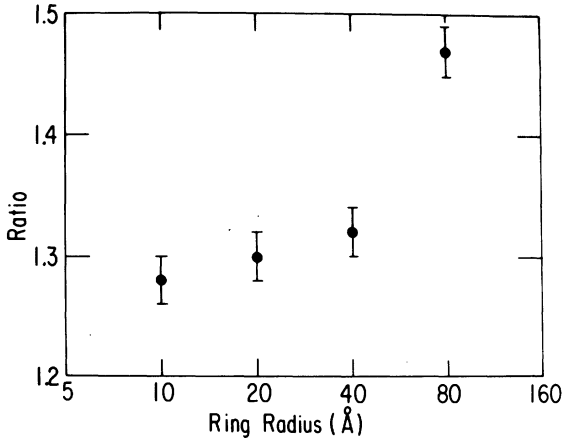

FIG. 12. Ratio of the exact cross section for ring-sphere entangling to that predicted by Eq. (27). The error bars represent the numerical accuracy of our determination of the cross section.

These complicated expressions are quoted here in full because those given by Rubinow and Keller contain several numerical errors.

The time derivative terms in Eqs. (A4) give the contribution of $\partial\Phi_I/\partial t+\partial\Phi_b(A)/\partial t$ to the total force. The velocity $\vec{v}_I$ at the center of the sphere is, from Eq. (A1),

$$\vec{v}_I(r=0)=(3/8\pi)^{1/2}(c_{1,-1}-c_{1,1})\hat{x} - i(3/8\pi)^{1/2}(c_{1,-1}+c_{1,1})\hat{y}+(3/4\pi)^{1/2}c_{1,0}\hat{z}\ . \tag{A6}$$

It follows immediately from Eqs. (A4) that the corresponding contribution to the total force is given by

$$\Delta\vec{F}=2\pi\rho b^3(\partial/\partial t)\vec{v}_I(r=0)\,. \tag{A7}$$

This is one of the assertions we wished to prove.

The problem of a moving sphere has two additional complications. First, Φ_b will have an additional time dependence because as the sphere occupies different positions in the fluid it will generate different boundary fields. Secondly, a velocity potential

$$\Phi_u=-\tfrac{1}{2}b^3\,\vec{U}\cdot(\vec{r}+\vec{U}t)/|\vec{r}+\vec{U}t\,|^3 \tag{A8}$$

representing the steadily moving sphere must be added. Both of these effects may be included in the formalism by writing

$$\Phi_b+\Phi_u=\sum_{n=1}^{\infty}\sum_{m=-n}^{n}\left(\frac{n}{n+1}c_{n,m}(t)+\frac{2n+1}{n+1}[c^{(1)}_{n,m}(t)+c^{(2)}_{n,m}(t)]\right)b^n\left(\frac{b}{r}\right)^{n+1}Y_n^m(\vartheta,\phi), \tag{A9}$$

where $c^{(1)}_{n,m}$ denotes the extra terms [corresponding to $\Phi_b(B)$] arising from the effects of the sphere motion on the boundary field, and $c^{(2)}_{n,m}$ denotes the extra terms arising from Φ_u. The force equations (A4) then still apply, provided $c_{n,m}$ is everywhere replaced by $c_{n,m}+c^{(1)}_{n,m}+c^{(2)}_{n,m}$. The force is to be evaluated at $t=0$ when the sphere is at the origin, and will contain terms of the type

$$(c_{n,m}+c^{(1)}_{n,m}+c^{(2)}_{n,m})(c_{j,k}+c^{(1)}_{j,k}+c^{(2)}_{j,k})$$

and of the type $(d/dt)(c_{1,m}+c^{(1)}_{1,m}+c^{(2)}_{1,m})$, evaluated at $t=0$. Contributions from $c_{n,m}c_{j,k}$ and from $dc_{1,m}/dt$ arise from the combination $\partial\Phi_I/\partial t+\partial\Phi_b(A)/\partial t+\frac{1}{2}(\vec{v}_I+\vec{v}_b)^2$, the first part of which we have already discussed. Terms of the type $c^{(2)}_{n,m}c^{(2)}_{j,k}$ and $dc^{(2)}_{1,m}/dt$ must combine to give zero, since a moving sphere alone will feel no force. Furthermore, $c^{(1)}_{n,m}=0$ at $t=0$. One is left with a contribution to the total force, which arises from $\partial\Phi_b(B)/\partial t+\vec{v}_u\cdot(\vec{v}_I+\vec{v}_b)$, and which is given by terms of the type $c_{n,m}c^{(2)}_{j,k}+c_{j,k}c^{(2)}_{n,m}$ and of the type $dc^{(1)}_{1,m}/dt$.

To find $c^{(2)}_{n,m}(0)$ one simply expands Φ_u in spherical harmonics. The only nonzero terms are

$$c^{(2)}_{1,1}=\tfrac{2}{3}(\tfrac{1}{6}\pi)^{1/2}(U_x-iU_y)\,,$$
$$c^{(2)}_{1,0}=-\tfrac{2}{3}(\tfrac{1}{3}\pi)^{1/2}U_z\,, \tag{A10}$$
$$c^{(2)}_{1,-1}=-\tfrac{2}{3}(\tfrac{1}{6}\pi)^{1/2}(U_x+iU_y)\ .$$

To determine $dc^{(1)}_{1,m}/dt$ at $t=0$, one needs to find the boundary field when the sphere is displaced an infinitesimal amount $\vec{U}t$ from the origin. The vortex potential Φ_I may be expressed in terms of a shifted coordinate system $\vec{r}'=\vec{r}-\vec{U}t$ centered on the displaced sphere by expanding

$$\Phi_I(\vec{r}'+\vec{U}t)=\Phi_I(\vec{r}')+\vec{U}t\cdot\nabla'\Phi_I(\vec{r}')\,, \tag{A11}$$

or

$$\Phi_I(\vec{r}'+\vec{U}t)=\left(1+U_x t\,\frac{\partial^++\partial^-}{2}+U_y t\,\frac{\partial^+-\partial^-}{2i} +U_z t\,\frac{\partial}{\partial z}\right)_{\vec{r}=\vec{r}'} \times\sum_{n=1}^{\infty}\sum_{m=-n}^{n}c_{n,m}r^nY_n^m(\vartheta,\phi)\,, \tag{A12}$$

where ∂^+, ∂^- are the ladder operators

$$\partial^{\pm}=\frac{\partial}{\partial x}\pm i\,\frac{\partial}{\partial y}\ . \tag{A13}$$

Using the known properties[33] of the ladder operators and of $\partial/\partial z$ acting on terms of the form $r^nY_n^m(\vartheta,\phi)$, the functional form of Φ_I in the shifted coordinate system can again be written as an expression of the type given in Eq. (A1),

$$\Phi_I=\sum_{n=1}^{\infty}\sum_{n=-m}^{m}c'_{n,m}r'^nY_n^m(\vartheta',\phi')\,. \tag{A14}$$

The boundary field generated by the shifted sphere, expressed in terms of the $\vec{r}'$ coordinate system, is then again of the form of Eq. (A2) with the $c_{n,m}$'s and the coordinates replaced by their primed counterparts. The resulting boundary field $\Phi_b(\vec{r}')$ can now be transformed back to the unprimed system using the same procedure, and the corrections to Eq. (A2) arising from the displacement of the sphere from the origin are then readily identified. From the definition of $c^{(1)}_{n,m}$ in Eq. (A9), one finds

$$c^{(1)}_{1,1} = -\sqrt{\tfrac{5}{9}}\,(U_x t + iU_y t)c_{2,2} + \sqrt{\tfrac{5}{9}}\,U_z t\, c_{2,1} + \sqrt{\tfrac{5}{54}}\,(U_x t - iU_y t)c_{2,0}\,,$$

$$c^{(1)}_{1,0} = -\sqrt{\tfrac{5}{18}}\,(U_x t + iU_y t)c_{2,1} + \sqrt{\tfrac{20}{27}}\,U_z t c_{2,0} + \sqrt{\tfrac{5}{18}}\,(U_x t + iU_y t)c_{2,-1}\,, \tag{A15}$$

$$c^{(1)}_{1,-1} = -\sqrt{\tfrac{5}{54}}\,(U_x t + iU_y t)c_{2,0} + \sqrt{\tfrac{5}{9}}\,U_z t\, c_{2,-1} + \sqrt{\tfrac{5}{9}}\,(U_x t - iU_y t)c_{2,-2}\,.$$

One can now evaluate the force contribution arising from $\partial\Phi_b(B)/\partial t + \vec{v}_u \cdot (\vec{v}_l + \vec{v}_b)$ by inserting $c_{n,m}c^{(2)}_{j,k} + c_{j,k}c^{(2)}_{n,m}$ into Eqs. (A4) in place of every term $c_{n,m}c_{j,k}$, and $dc^{(1)}_{1,m}/dt$ in place of every term $dc_{1,m}/dt$. Given the results of Eqs. (A10) and (A15), a little algebra is sufficient to show that the result is identically zero. This is the second assertion we needed to prove.

---

*Supported in part by the Louis Block Fund, The University of Chicago. We have also benefitted from support of the Materials Research Laboratory by the National Science Foundation.

[1]G. W. Rayfield and F. Reif, Phys. Rev. 136, 1194 (1964).
[2]H. E. Hall and W. F. Vinen, Proc. R. Soc. A 238, 204 (1956).
[3]H. E. Hall, Philos. Mag. Suppl. 9, 89 (1960).
[4]G. W. Rayfield, Phys. Rev. 168, 222 (1968).
[5]G. Gamota and M. Barmatz, Phys. Rev. Lett. 22, 874 (1969).
[6]A. L. Fetter, Phys. Rev. A 6, 402 (1972).
[7]G. Gamota and T. M. Sanders, Jr., Phys. Rev. Lett. 15, 949 (1965).
[8]A. Walraven, Phys. Rev. A 1, 145 (1970).
[9]For a review of experimental work on this effect see R. J. Donnelly and P. H. Roberts, Proc. R. Soc. A 312, 519 (1969). Also see W. P. Pratt, Jr., and W. Zimmermann, Jr., Phys. Rev. 177, 412 (1969).
[10]K. W. Schwarz, Phys. Rev. 165, 323 (1967).
[11]G. Gamota and T. M. Sanders, Jr., Phys. Rev. Lett. 21, 200 (1968).
[12]G. Careri, S. Cunsolo, P. Mazzoldi, and M. Santini, Phys. Rev. Lett. 5, 392 (1965).
[13]G. W. Rayfield, Phys. Rev. 168, 222 (1968).
[14]R. J. Donnelly and P. H. Roberts, Philos. Trans. R. Soc. Lond. A 271, 41 (1971).
[15]K. W. Schwarz and P. S. Jang, Phys. Rev. A 8, 3199 (1973).
[16]G. Gamota, Phys. Rev. Lett. 31, 517 (1973).
[17]T. C. Padmore, Phys. Rev. Lett. 28, 469 (1972).
[18]If a beam of vortex rings passes through the vortex lines filling a rotating bucket, some of the rings in the beam disappear, presumably as the result of close encounters with vortex lines. Similarly, charge carriers crossing a rotating bucket may become trapped on the lines.
[19]E. R. Huggins, Phys. Rev. A 1, 327 (1970).
[20]A. L. Fetter, *The Physics of Liquid and Solid Helium*, edited by K. H Benneman and J. B. Ketterson (Wiley, New York, 1974).
[21]K. W. Schwarz, Adv. Chem. Phys. (to be published).
[22]W. J. Titus, Phys. Rev. A 2, 206 (1970).
[23]S. E. Goodman, Phys. Fluids 14, 1293 (1971).
[24]G. K. Batchelor, *An Introduction to Fluid Dynamics* (Cambridge University, Cambridge, 1970).
[25]It should be noted that $d\vec{v}_l$ is not a field which can exist by itself, since an element $d\vec{l}$ cannot exist by itself.
[26]I. S. Gradshteyn and I. M. Ryzhik, *Tables of Integrals, Series, and Products* (Academic, New York, 1965). Formula 7.225.4 can be transformed into the desired expression by setting $a = \cosh 2p$ and differentiating with respect to a.
[27]Reference 24, p. 273.
[28]Reference 24, p. 509.
[29]R. J. Arms and F. R. Hama, Phys. Fluids 8, 553 (1965).
[30]W. I. Glaberson and M. Steingart, Phys. Rev. Lett. 26, 1423 (1971).
[31]Reference 24, p. 404.
[32]S. I. Rubinow and J. B. Keller, Phys. Fluids 14, 1302 (1971).
[33]G. Goertzel and N. Tralli, *Some Mathematical Methods of Physics* (McGraw-Hill, New York, 1960), Chap. 11.